Substellar Companions to Evolved Intermediate-Mass Stars: HD 145457 and HD 180314

Sato, Bun'ei ; Omiya, Masashi ; Yujuan, Liu ; Harakawa, Hiroki ; Izumiura, Hideyuki ; Kambe, Eiji ; Toyota, Eri ; Murata, Daisuke ;…

(Citation)
Publications of the Astronomical Society of Japan,62(4):1063-1069

(Issue Date)
2010-08-25

(Resource Type)
journal article

(Version)
Accepted Manuscript

Substellar Companions to Evolved Intermediate-Mass Stars: HD 145457 and HD 180314

Bun'ei SATO,[1] Masashi OMIYA,[2] Yujuan LIU,[3] Hiroki HARAKAWA,[4] Hideyuki IZUMIURA,[5,6] Eiji KAMBE,[5] Eri TOYOTA,[7] Daisuke MURATA,[8] Byeong-Cheol LEE,[2,9] Seiji MASUDA,[10] Yoichi TAKEDA,[6,11] Michitoshi YOSHIDA,[12] Yoichi ITOH,[8] Hiroyasu ANDO,[6,11] Eiichiro KOKUBO,[6,11] Shigeru IDA,[4] Gang ZHAO,[13] and Inwoo HAN[2]

[1] *Global Edge Institute, Tokyo Institute of Technology, 2-12-1-S6-6 Ookayama, Meguro-ku, Tokyo 152-8550, Japan*

sato.b.aa@m.titech.ac.jp

[2] *Korea Astronomy and Space Science Institute, 61-1 Hwaam-dong, Yuseong-gu, Daejeon 305-348, Korea*

[3] *Key Laboratory of Optical Astronomy, National Astronomical Observatories, Chinese Academy of Sciences, A20 Datun Road, Chaoyang District, Beijing 100012, China*

[4] *Department of Earth and Planetary Sciences, Tokyo Institute of Technology, 2-12-1 Ookayama, Meguro-ku, Tokyo 152-8551, Japan*

[5] *Okayama Astrophysical Observatory, National Astronomical Observatory of Japan, Kamogata, Okayama 719-0232, Japan*

[6] *The Graduate University for Advanced Studies, Shonan Village, Hayama, Kanagawa 240-0193, Japan*

[7] *Kobe Science Museum, 7-7-6 Minatoshima-Nakamachi, Chuo-ku, Kobe, Hyogo 650-0046*

[8] *Graduate School of Science, Kobe University, 1-1 Rokkodai, Nada, Kobe 657-8501, Japan*

[9] *Department of Astronomy and Atmospheric Sciences, Kyungpook National University, Daegu 702-701, Korea*

[10] *Tokushima Science Museum, Asutamu Land Tokushima, 45-22 Kibigadani, Nato, Itano-cho, Itano-gun, Tokushima 779-0111, Japan*

[11] *National Astronomical Observatory of Japan, 2-21-1 Osawa, Mitaka, Tokyo 181-8588, Japan*

[12] *Hiroshima Astrophysical Science Center, Hiroshima University, Higashi-Hiroshima, Hiroshima 739-8526, Japan*

[13] *National Astronomical Observatories, Chinese Academy of Sciences, A20 Datun Road, Chaoyang District, Beijing 100012, China*

(Received ; accepted)

Abstract

We report the detections of two substellar companions orbiting around evolved intermediate-mass stars from precise Doppler measurements at Subaru Telescope and

Okayama Astrophysical Observatory. HD 145457 is a K0 giant with a mass of 1.9 $M_\odot$ and has a planet of minimum mass $m_2 \sin i = 2.9 M_{\rm J}$ orbiting with period of $P = 176$ d and eccentricity of $e = 0.11$. HD 180314 is also a K0 giant with 2.6 $M_\odot$ and hosts a substellar companion of $m_2 \sin i = 22 M_{\rm J}$, which falls in brown-dwarf mass regime, in an orbit with $P = 396$ d and $e = 0.26$. HD 145457 b is one of the innermost planets and HD 180314 b is the seventh candidate of brown-dwarf-mass companion found around intermediate-mass evolved stars.

Key words: stars: individual: HD 145457 — stars: individual: HD 180314 — planetary systems — techniques: radial velocities

1. Introduction

Over 400 exoplanets have been discovered by various techniques during the past 15 years[1]. Among the techniques, precise Doppler technique has been the most powerful method for planet detection around various types of stars including solar-type stars, evolved giants and subgiants, early-type stars, and so on (e.g. Udry & Santos 2007 and references therein). Recently, precise Doppler measurements in infrared wavelength region started to explore planets around very low-mass stars down to 0.1 $M_\odot$ (Bean et al. 2010). These surveys will help us to understand properties of planets as a function of stellar mass, age, evolutionary stage, and so on, and thus provide us more general picture of planet formation and evolution.

In particular, planets around giants and subgiants have been extensively surveyed over the past several years mainly from the viewpoint of planet searches around intermediate-mass (1.5–5$M_\odot$) stars (e.g. Frink et al. 2002; Setiawan et al. 2005; Sato et al. 2008b; Hatzes et al. 2005, 2006; Johnson et al. 2010; Lovis & Mayor 2007; Niedzielski et al. 2009b; Döllinger et al. 2009; de Medeiros et al. 2009; Liu et al. 2009; Omiya et al. 2009). Intermediate-mass dwarfs, namely BA-type dwarfs, are more difficult for Doppler planet searches because of paucity of spectral features and their rotational broadening. It is thus difficult to achieve high measurement precision in radial velocity (but see eg. Galland et al. 2005, 2006). On the other hand, those in evolved stages, namely GK-type giants and subgiants, have many sharp absorption lines in their spectra suitable for precise radial velocity measurements, which makes them promising targets for Doppler planet searches. Actually, more than 30 substellar companions to such evolved stars have been already found and they have shown remarkable properties: more than twice higher occurrence rate of giant planets for intermediate-mass subgiants than that for lower-mass stars (Johnson et al. 2007b; Bowler et al. 2010), larger typical mass of giant planets (Lovis et al. 2007; Omiya et al. 2009), lack of inner planets with semimajor axes $<$0.6 AU (Johnson et al. 2007a; Sato et al. 2008a; Niedzielski et al. 2009a),

[1] See, e.g., table at http://exoplanet.eu/

and lack of metal-rich tendency in host stars (Pasquini et al. 2007; Takeda et al. 2008). All these statistical properties should be confirmed by collecting a larger number of samples.

Since 2001, we have been carrying out a Doppler planet search program targeting 300 GK giants at Okayama Astrophysical Observatory (OAO) and have discovered 9 planets and 1 brown dwarf so far from the program (Sato et al. 2003, 2007, 2008ab; Liu et al. 2008). In order to further extend the survey, we have established an international consortium between Chinese, Korean, and Japanese researchers using 2m class telescopes in the three countries (East-Asian Planet Search Network; Izumiura 2005), which recently announced discoveries of a planet (Liu et al. 2009) and a brown dwarf (Omiya et al. 2009) around GK giants. A total of about 600 GK giants are now under survey by the consortium.

In this paper, we report the detections of two new substellar companions around intermediate-mass giants (HD 145457 and HD 180314) from our newly started planet search program using Subaru 8.2m telescope and the above 2m class telescopes. The substellar companions presented here were uncovered by the initial screening with Subaru and followed up with OAO 1.88m telescope. We describe the outline of the Subaru survey in Section 2 and the observations in Section 3. The stellar properties are presented in Section 4, and radial velocities, orbital solutions, and results of line shape analysis are provided in Section 5. Section 6 is devoted to summary and discussion.

2. Subaru Survey for Planets around GK Giants

The main purpose of the Subaru program is to quickly identify planet-hosting candidates from hundreds of sample stars taking advantage of the large telescope aperture. Our basic strategy is thus to observe each star three times in a semester with an interval of about 1.5 months for the first screening to identify stars showing large radial velocity variations. Since it is known that planets with periods less than 130 days seem to be rare around giants, we focus on the detection of planets with longer periods at first. For stars which turn out to show large radial velocity variations, we conduct follow-up observations using 1.8m telescope at Bohyunsan Optical Astronomy Observatory (BOAO; Korea), 2.16m telescope at Xinglong station (China), and 1.88m telescope at OAO (Japan) to confirm their periodicity. For this purpose, our science targets are typically brighter than visual magnitude $V = 7$, which are barely observable using the 2m class telescopes with a Doppler precision of $\lesssim 10$ m s^{-1}.

Our survey targets for Subaru are selected from the Hipparcos catalogue (ESA 1997) according to the following criteria, which are basically the same as those for individual planet searches at BOAO, Xinglong, and OAO except for visual magnitude: stars with 1) $6.5 \leq V < 7$ to attain a sufficient signal-to-noise ratio (S/N) to achieve a precision of $\lesssim 10$ m s^{-1} even using 2m class telescopes, 2) a color index of $0.6 \lesssim B - V \lesssim 1.0$ to achieve intrinsic radial velocity stability to a level of $\sigma \lesssim 20$ m s^{-1}, 3) an absolute magnitude of $-3 \lesssim M_V \lesssim 2.5$ to include stars with masses of 1.5–5$M_{\odot}$, and 4) a declination of $\delta > -25°$ to be observed from all 4 sites mentioned above.

We conducted the first observation in 2006 at Subaru and completed the initial screening for about 300 stars in the last 4 years.

3. Observations and Radial Velocity Analysis

We obtained a total of 3 spectra for each of HD 145457 and HD 180314 in 2006 April, May, and July using High Dispersion Spectrograph (HDS; Noguchi et al. 2002) equipped with Subaru. We used an iodine absorption cell (I_2 cell; Kambe et al. 2002) to provide fiducial wavelength reference for precise radial velocity measurement. We adopted the setup of StdI2b in the first two runs and StdI2a in the third one, which covers a wavelength region of 3500–6200 Å and 4900–7600 Å, respectively, in order to inspect as many absorption lines as possible for stellar abundance analysis. The slit width was set to $0''.6$, giving a wavelength resolution ($\lambda/\Delta\lambda$) of 60,000. Typical signal-to-noise ratio (S/N) was 150–230 pix^{-1} for HD 145457 and 100–170 pix^{-1} for HD 180314 with an exposure time of 45–180 sec depending on weather condition.

After the observations at Subaru, we found that the stars showed large radial velocity variations with $\sigma > 45$ m s^{-1} and then started follow-up observations using 1.88m telescope with High Dispersion Echelle spectrograph (HIDES; Izumiura 1999) at OAO. We collected a total of 23 and 21 data points for HD 145457 and HD180314, respectively, from March 2008 to March 2010. The wavelength region was set to cover 3750–7500 Å using RED cross-disperser and the slit width was set to $0''.78$, giving a wavelength resolution of 67,000 by about 3.3 pixels sampling. We used an I_2 cell for precise radial velocity measurement and also took pure stellar spectra without I_2 cell for abundance analysis. Typical S/N was 170 pix^{-1} for both stars with an exposure time of 1500 sec. The reduction of echelle data for HDS and HIDES was performed using the IRAF [2] software package in the standard manner.

For precise Doppler analysis, we basically adopted the modeling technique of an I_2-superposed stellar spectrum (star+I_2) detailed in Sato et al. (2002), which is based on the method by Butler et al. (1996). In the technique, a star+I_2 spectrum is modeled as a product of a high resolution I_2 and a stellar template spectrum convolved with a modeled instrumental profile (IP) of the spectrograph. The IP is modeled with a combination of a central and several satellite Gaussian profiles which are placed at appropriate intervals and have suitable widths, depending on the properties of the spectrograph (e.g. Valenti et al. 1995; Sato et al. 2002). To obtain the stellar template, Sato et al. (2002) extracted a high resolution stellar spectrum from several star+I_2 spectra. However, when we applied the technique to the HDS data, we found that systematic errors sometimes appeared in radial velocities derived by using thus

[2] IRAF is distributed by the National Optical Astronomy Observatories, which is operated by the Association of Universities for Research in Astronomy, Inc. under cooperative agreement with the National Science Foundation, USA.

obtained template. We finally found that such systematic errors disappeared when we used a stellar template derived from a HIDES spectrum that was obtained by deconvolving a pure stellar spectrum with the spectrograph IP estimated from a B-star+I_2 spectrum. Therefore, we decided to use the same stellar template thus obtained from HIDES data for the radial velocity analysis of both HDS and HIDES data.

4. Stellar Properties

HD 145457 (HIP 79219) is listed in the Hipparcos catalog as a K0 III giant star with a magnitude $V = 6.57$ and a color index $B - V = 1.037$. The Hipparcos parallax $\pi = 7.93 \pm 0.73$ mas corresponds to a distance of 126±12 pc, an absolute magnitude $M_V = 0.967$. The color excess $E(B - V)$ was calibrated according to Beer et al. (2002), and the interstellar extinction $A_V = 0.099$. The effective temperature $T_{\rm eff} = 4757 \pm 100$K was derived from the color index $B - V$ and metallicity [Fe/H] using the calibration of Alonso et al. (2001), and a bolometric correction $B.C. = -0.354$ was derived from the calibration of Alonso et al. (1999) depending on temperature and metallicity. Then the stellar luminosity was estimated to $L = 45.2 \pm 8.2 L_\odot$, and a radius to $R = 9.9 \pm 0.5 R_\odot$. Stellar mass $M = 1.9 \pm 0.3 M_\odot$ was estimated from the evolutionary tracks of Yonsei-Yale (Yi et al. 2003). Surface gravity $\log g = 2.77 \pm 0.1$ was determined via Hipparcos parallaxes (ESA 1997). Iron abundance was determined from the equivalent widths measured from a pure stellar spectrum taken with HIDES (5000–6100 and 6000–7100 Å) combined with the model atmosphere (Kurucz 1993). Microturbulent velocity were obtained by forcing Fe I lines with different strengths to give the same abundances. We iterated the whole procedure described above until the final metallicity from the measured equivalent widths became consistent with the one input as an initial guess. Finally we got $[{\rm Fe/H}] = -0.14 \pm 0.09$ and a microturbulent velocity $v_t = 1.3 \pm 0.2$ km s^{-1}.

HD 180314 (HIP 94576) is also a K0 III giant star with $V = 6.61$ and $B - V = 1.000$. The Hipparcos parallax $\pi = 7.59 \pm 0.64$ mas yields a distance of 132±11 pc and $M_V = 0.931$, $A_V = 0.081$. The atmospheric parameters for the star were derived by the same procedure as described above to be $T_{\rm eff} = 4917 \pm 100$ K, $\log g = 2.98 \pm 0.1$, $v_t = 1.1 \pm 0.2$ km s^{-1}, $[{\rm Fe/H}] = 0.2 \pm 0.09$, and other stellar parameters were $L = 44.0 \pm 7.2 L_\odot$, $R = 9.2 \pm 0.4 R_\odot$, $B.C. = -0.289$ and $M = 2.6 \pm 0.3 M_\odot$. Although we have not obtained projected rotational velocities for the stars, absorption lines of HD180314 are obviously narrower and deeper than those of HD 145457, which resulted in better precision in radial velocity measurements for HD 180314 than for HD 145457 even with nearly the same S/N (see section 5.1 and tables 2–3).

Hipparcos made a total of 229 and 130 observations of HD 145457 and HD 180314, respectively, and revealed a photometric stability down to $\sigma = 0.009$ mag for both stars. Ca II H K lines of HD 145457 show no significant emission in the line cores, but those of HD 180314 show a slight core reversal, suggesting that the star is slightly chromospherically active. However, as shown in Figure 1, the reversal of HD 180314 is not significant compared to those of other chromospherically active stars in our sample, such as HD 120048 (Figure 1), which exhibits a velocity scatter of about 20 m s^{-1} at most. Thus, the intrinsic radial velocity "jitter" of HD 180314 is probably expected to be no larger than that of HD 120048, which is consistent with the RMS scatters of the residuals to the Keplerian fit for the star (see Section 5).

5. Results

5.1. Radial Velocities and Orbital Solutions

The observed radial velocities for HD 145457 and HD 180314 are shown in Figure 2 and 3, and are listed in Table 2 and 3, respectively, together with their estimated uncertainties. Each uncertainty was derived from an ensemble of velocities from individual ∼400 spectral segments (each 3Å long) of each exposure. Lomb-Scargle periodogram (Scargle 1982) of the data for HD 145457 and HD 180314 exhibits a dominant peak at a period of 176 days and 388 days, respectively. False Alarm Probability (FAP) of the peaks were estimated by using a bootstrap randomization method in which the observed radial velocities were randomly redistributed, keeping the observation time fixed. We generated 10^5 fake datasets in this way, and applied the same periodogram analysis to them. Since no fake datasets exhibited a periodogram power higher than the observed ones, the FAPs are less than 1×10^{-5}.

The best-fit Keplerian orbits for the stars were derived from the combined sets of the Subaru and OAO data using a Levenberg-Marquardt fitting algorithm to obtain a minimum chi-squared solution by varying the free parameters (orbital period, time of periastron passage, eccentricity, velocity amplitude and argument of periastron). No velocity offsets were applied between the Subaru and OAO data because we used the same stellar template to derive radial velocities (see in Section 2). The resulting Keplerian models are shown in Figure 2 and 3 overplotted on the velocities, and their parameters are listed in Table 4.

The radial velocities of HD 145457 can be well fitted by an orbit with a period $P = 176.30 \pm 0.39$ days, a velocity semiamplitude $K_1 = 70.6 \pm 3.1$ m s^{-1}, and an eccentricity $e = 0.112 \pm 0.035$. The rms scatter of the residuals to the Keplerian fit was 9.7 m s^{-1} and the reduced $\sqrt{\chi^2}$ was 1.8. The uncertainty for each orbital parameter was determined using a bootstrap Monte Carlo approach, subtracting the theoretical fit, scrambling the residuals, adding the theoretical fit back to the residuals and then refitting. Adopting a stellar mass of $1.9 M_{\odot}$, we obtain a minimum mass for the companion of $m_2 \sin i = 2.9 M_{\rm J}$ and a semimajor axis of $a = 0.76$ AU.

The radial velocity variations of HD 180314 can be well reproduced by a Keplerian orbit with $P = 396.03 \pm 0.62$ days, $K_1 = 340.8 \pm 3.3$ m s^{-1}, and $e = 0.257 \pm 0.010$. The uncertainty of each parameter was estimated using the same method as described above. Adopting a stellar mass of 2.6 $M_{\odot}$, we obtain a minimum mass for the companion $m_2 \sin i = 22 M_{\rm J}$ and a semimajor axis $a = 1.4$ AU. The rms scatter of the residuals to the Keplerian fit was 12.9 m s^{-1} and the reduced $\sqrt{\chi^2}$ was 3.1. As seen in Figure 3, we found that the residuals showed possible non-random variability. Periodogram analysis for the residuals exhibits a peak around 112 days as shown in Figure 4, but the peak is not considered to be significant at this stage because of the high FAP value (14%). When we assume the periodicity is originated from rotational modulation, the period corresponds to stellar rotational velocity of about 4 km s^{-1}. The value is slightly large compared with those of typical GK giants (see Figure 10 in Takeda et al. 2008), but is still possible taking account of the moderate stellar activity of this star. More frequent observations will enable us to confirm the periodicity and clarify the origin, stellar activity or additional companion.

5.2. *Line Shape Analysis*

We performed spectral line shape analysis by using high resolution stellar templates to investigate other possible causes producing apparent radial velocity variations such as pulsation and rotational modulation rather than orbital motion. For this purpose, we followed a procedure described in Sato et al. (2007), in which we used high resolution I_2-free stellar templates extracted from several star+I_2 spectra. Details of the template extraction technique are described in Sato et al. (2002).

At first, we extracted two stellar templates from five star+I_2 spectra at the peak and valley phases of observed radial velocities for each star. Then, cross correlation profiles of the two templates were calculated for about 80 spectral segments (4–5Å width each) in which severely blended lines or broad lines were not included. Three bisector quantities were calculated for the cross correlation profile of each segment: the velocity span (BVS), which is the velocity difference between two flux levels of the bisector; the velocity curvature (BVC), which is the difference of the velocity span of the upper half and lower half of the bisector; and the velocity displacement (BVD), which is the average of the bisector at three different flux levels. We used flux levels of 25%, 50%, and 75% of the cross correlation profile to calculate the above three bisector quantities. As a result, both of the BVS and the BVC for the stars were identical to zero, which means that the cross correlation profiles are symmetric, and the average BVD agreed with the velocity difference between the two templates at the peak and valley phases of observed radial velocities ($\simeq 2K_1$). These results mean that the observed radial velocity variations are due to parallel shifts of the spectral lines and are thus consistent with the planetary hypothesis. Resulting bisector quantities are summarized in Table 5.

6. Summary and Discussion

We here reported the two new substellar companions to K0 III giants from Subaru and OAO planet search programs. The discoveries add to the recent growing population of substellar companions around evolved intermediate-mass stars.

HD 145457 b ($m_2 \sin i = 2.9 M_{\rm J}$, $a = 0.76$ AU) is one of the innermost planets found around giants. All the planets currently known around evolved intermediate-mass stars orbit at a≥0.6 AU (Johnson et al. 2007a; Sato et al. 2008a; Niedzielski et al. 2009a). Two possible causes of the lack of inner planets has been proposed: they are originally deficient or engulfed by the central stars. In the case of intermediate-mass subgiants ($< 2M_\odot$), the former scenario is considered to be appropriate because they are obviously less evolved and have stellar radii of $\lesssim 6R_\odot$, which means that they could only have engulfed very short-period planets like hot-Jupiters (e.g. Johnson et al. 2007a). It is not easy, however, to discriminate between the two scenarios in the case of intermediate-mass giants (typically $\geq 2M_\odot$) because it is difficult to know accurate evolutionary status of giants. The inner planets could be tidally engulfed by the central stars at the phase of the tip of red giant branch (RGB). Thus if we observe giants that have already passed through the tip of RGB, namely core-helium burning stars, we could not find any inner planets around the stars even if the planets originally existed (Sato et al. 2008a; Villaver & Livio 2009). However, it is apparently difficult to distinguish such giants from those ascending RGB for the first time because they locate at nearly the same region on the HR diagram (red clump region). Based on stellar evolutionary models (cf.evolutionary tracks by Girardi et al. 2000), core-helium burning giants stay at the clump region for ~100 times longer than first ascending RGB stars do. Therefore, if we can collect hundreds of planets around such giants, it will become possible to verify the causes of the lack of inner planets statistically.

HD 180314 b has a minimum mass of 22 M_J and orbits around the central star with $2.6M_\odot$. This is the 7 th brown-dwarf-mass (13–$80M_J$) companion to evolved intermediate-mass stars (Hatzes et al. 2005; Lovis & Mayor 2007; Liu et al. 2008; Omiya et al. 2009; Niedzielski et al. 2009b[3]). Actually all of their host stars are estimated to be more massive than 2.5 $M_\odot$, suggesting that more massive stars tend to have more massive companions (Lovis & Mayor 2007; Omiya et al. 2009). Several scenarios have been proposed for the formation of brown-dwarf-mass companions including gravitational collapse in protostellar clouds like stellar binary systems (Bonnell & Bastien 1992; Bate 2000) and gravitational instability in protostellar disks (Boss 2000; Rice et al. 2003). Even by core-accretion scenario in protoplanetary disks, super-massive companions with $\gtrsim 10M_J$ could be formed on a certain truncation condition for gas accretion (Ida & Lin 2004; Alibert et al. 2004; Mordasini et al. 2007). If the companions form like stellar binary systems, they are expected to have a wide variety of orbital eccentricity. The above 7 brown dwarf candidates, however, have relatively low eccentricies of 0–0.3, which may be favored by the scenarios that they formed in circumstellar disks and have not experienced significant gravitational interaction with other companions. One more thing to note here is that metallicity of the host stars of the above brown dwarf candidates are ranging from [Fe/H] $= -1$ to 0.2. Although the number of samples is still small, this suggests that the formation mechanism is independent of or less sensitive to metallicity in this range.

[3] BD+20 2457 has two brown-dwarf-mass companions in the system.

This research is based on data collected at Subaru Telescope and Okayama Astrophysical Observatory (OAO), which are operated by National Astronomical Observatory of Japan (NAOJ). We are grateful to all the staff members of Subaru and OAO for their support during the observations. We thank the National Institute of Information and Communications Technology for their support on high-speed network connection for data transfer and analysis. BS is supported by MEXT's program "Promotion of Environmental Improvement for Independence of Young Researchers" under the Special Coordination Funds for Promoting Science and Technology, and by Grant-in-Aid for Young Scientists (B) No.20740101 from the Japan Society for the Promotion of Science (JSPS). YJL is supported by the National Natural Science Foundation of China under grant number 10803010 and 10821061. BCL acknowledge the Astrophysical Research Center for the Structure and Evolution of the Cosmos (ARCSEC, Sejong University) of the Korea Science and Engineering Foundation (KOSEF) through the Science Research Center (SRC) program. This research has made use of the SIMBAD database, operated at CDS, Strasbourg, France.

References

Alonso, S., Arribas S., Martínez-Roger C., 1999, A&AS, 140, 261

Alonso, S., Arribas S., Martínez-Roger C., 2001, A&A, 376, 1039

Alibert, Y., Mordasini, C., Benz, W., Winisdoerffer, C. 2005, A&A, 434, 343

Bate, M. R. 2000, MNRAS, 314, 33

Bean, J.L., et al. 2010, ApJ, in press (arXiv:0911.3148v2)

Beers T. C. et al. 2002, AJ, 124, 931

Bonnell, I. & Bastien, P. 1992, ApJ, 401, 654

Boss, A. P. 2000, ApJ, 536, L101

Bowler, B.P., et al., ApJ, 710, 1365

Butler, R.P., et al. 2006, ApJ, 646, 505

Chen, Y.Q., Nissen, P.E., Zhao, G., Zhang, H.W., & Benoni, T., 2000, A&AS, 141, 491

de Medeiros, J.R., et al., A&A, 504, 617

Döllinger, M.P., Hatzes, A.P., Pasquini, L., Guenther, E.W., & Hartmann, M. 2009, A&A, 505, 1311

ESA. 1997, The *Hipparcos* and Tycho Catalogues (ESA SP-1200; Noordwijk: ESA) A&A, 394, 5

Frink, S., Mitchell, D.S., Quirrenbach, A., Fischer, D., Marcy, G.W., & Butler, R.P. 2002, ApJ, 576, 478

Galland, F., Lagrange, A.-M., Udry, S., Chelli, A., Pepe, F., Beuzit, J.-L., & Mayor, M. 2005, A&A, 444, L21

Galland, F., Lagrange, A.-M., Udry, S., Beuzit, J.-L., Pepe, F., & Mayor, M. 2006, A&A, 452, 709

Girardi, L., Bressan, A., Bertelli, G., & Chiosi, C. 2000, A&AS, 141, 371

Hatzes, A.P., Guenther, E.W., Endl, M., Cochran, W.D., Döllinger, M.P., & Bedalov, A. 2005, A&A, 437, 743

Hatzes, A.P., et al. 2006, A&A, 457, 335
Ida, S. & Lin, D.N.C. 2004, ApJ, 616, 567
Izumiura, H. 1999, in Proc. 4th East Asian Meeting on Astronomy, ed. P.S. Chen (Kunming: Yunnan Observatory), 77
Izumiura, H. 2005, JKAS, 38, 81
Johnson, J.A., et al. 2007a, ApJ, 665, 785
Johnson, J.A., et al. 2007b, ApJ, 670, 833
Johnson, J.A., et al. 2010, PASP, in press (arXiv:1003.3445v1)
Kambe, E., et al. 2002, PASJ, 54, 865
Kurucz, R. L. 1993, Kurucz CD-ROM, No. 13 (Harvard-Smithsonian Center for Astrophysics)
Liu, Y.-J., et al. 2008, ApJ, 672, 553
Liu, Y.-J., Sato, B., Zhao, G., & Ando, H. 2009, RAA, 9, L1
Lovis, C., & Mayor, M. 2007, A&A, 472, 657
Mordasini, C., Alibert, Y., Benz, W., & Naef, D. 2007, in "Extreme Solar Systems", ASP Conf. Ser. Vol. 398, 235
Niedzielski, A., Gozdziewski, K., Wolszczan, A., Konacki, M., Nowak, G., & Zielinski, P. 2009a, ApJ, 693, 276
Niedzielski, A., Nowak, G., Adamow, M., & Wolszczan, A. 2009b, ApJ, 707, 768
Noguchi, K., et al. 2002, PASJ, 54, 855
Omiya, M., et al., 2009, PASJ, 61, 825
Pasquini, L., et al. 2007, A&A, 473, 979
Rice, W.K.M., Armitage, P.J., Bonnell, I.A., Bate, M.R., Jeffers, S.V., & Vine, S.G., 2003, MNRAS, 346, L36
Sato, B., Kambe, E., Takeda, Y., Izumiura, H., & Ando, H. 2002, PASJ, 54, 873
Sato, B., et al. 2003, ApJ, 597, L157
Sato, B., Kambe, E., Takeda, Y., Izumiura, H., Masuda, S., & Ando, H. 2005, PASJ, 57, 97
Sato, B., et al. 2007, ApJ, 661, 527
Sato, B., et al. 2008a, PASJ, 60, 539
Sato, B., et al. 2008b, PASJ, 60, 1317
Scargle, J. D. 1982, ApJ, 263, 835
Setiawan, J., et al. 2005, A&A, 437, 31
Takeda, Y., Sato, B., & Murata, D., 2008, PASJ, 60, 781
Udry, S. & Santos, N.C. 2007, ARA&A, 45, 397
Valenti, J.A., Butler, R.P., & Marcy, G.W. 1995, PASP, 107, 966
Villaver, E. & Livio, M. 2009, ApJ, 705, L81
Yi, S. K., Kim, Y. C., & Demarque, P., 2003, ApJS, 144, 259

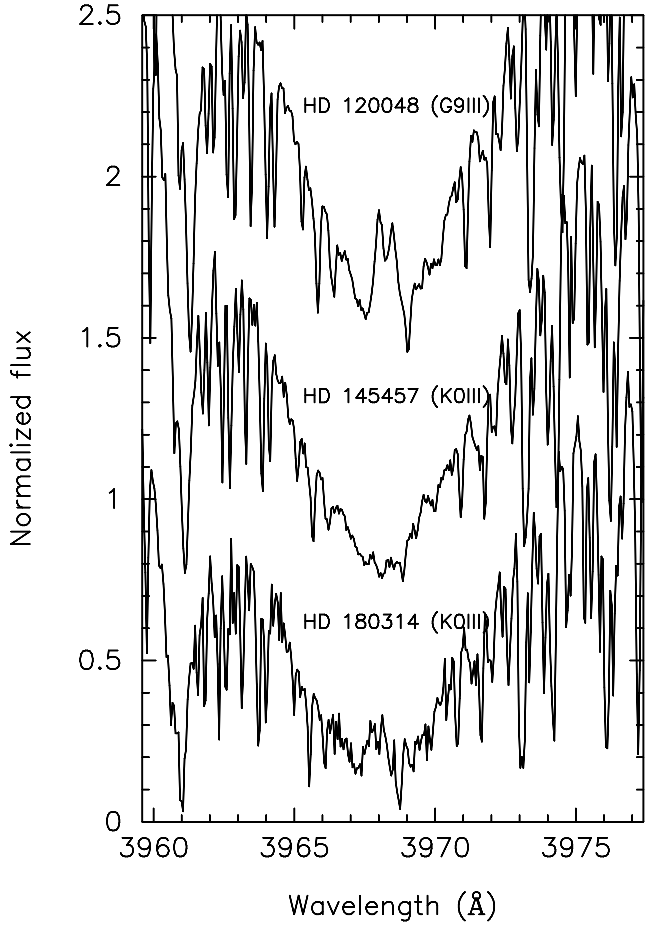

Fig. 1. Spectra in the region of Ca H lines. HD 180314 exbihits a slight core reversal in the line, but it is not significant compared to that in the chromospheric active star HD 120048, which shows velocity scatter of about 20 m s^{-1}. A vertical offset of about 0.7 is added to each spectrum.

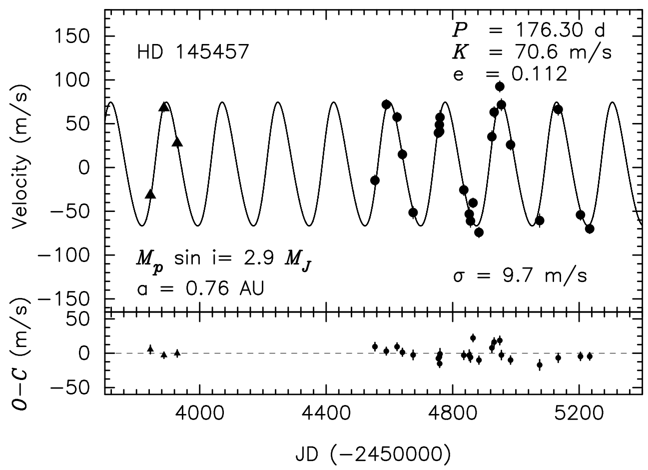

Fig. 2. *Top*: Radial velocities of HD 145457 observed at Subaru (triangles) and OAO (dots). The Keplerian orbital fit is shown by the solid line. *Bottom*: Residuals to the Keplerian fit. The rms to the fit is 9.7 m s^{-1}.

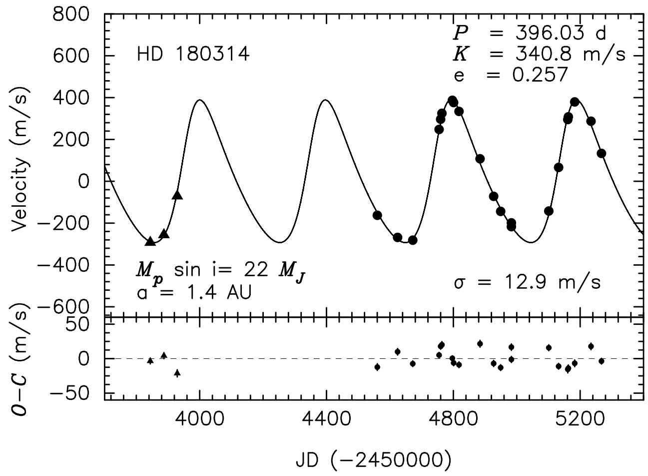

Fig. 3. *Top*: Radial velocities of HD 180314 observed at Subaru (triangles) and OAO (dots). The Keplerian orbital fit is shown by the solid line. *Bottom*: Residuals to the Keplerian fit. The rms to the fit is 12.9 m s^{-1}.

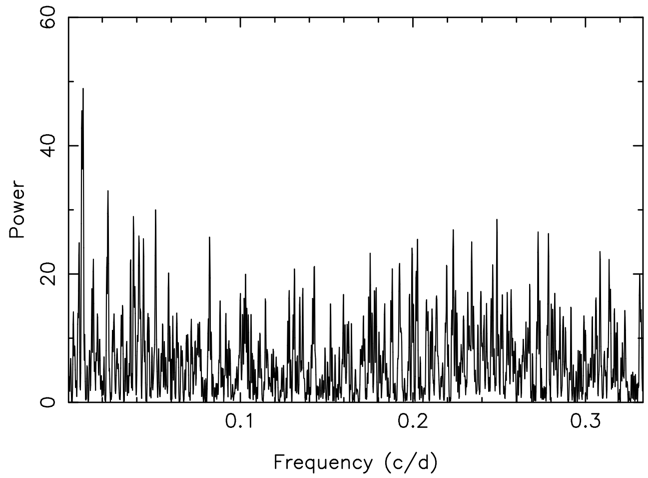

Fig. 4. Periodogram of the residuals to the Keplerian fit for HD 180314. A possible peak ($FAP = 0.14$) is seen at a period of 112 days (0.0089 cycle d^{-1}).

Table 1. Stellar parameters

Parameter	HD 145457	HD 180314
Sp. Type	K0	K0
π (mas)	7.93±0.73	7.59±0.64
V	6.57	6.61
$B-V$	1.037	1.000
A_V	0.099	0.081
M_V	0.967	0.931
$B.C.$	−0.354	−0.289
$T_{\rm eff}$ (K)	4757±100	4917±100
$\log g$	2.77±0.1	2.98±0.1
v_t	1.3±0.2	1.1±0.2
[Fe/H]	−0.14±0.09	+0.20±0.09
L ($L_\odot$)	45.2±8.2	44.0±7.2
R ($R_\odot$)	9.9±0.5	9.2±0.4
M ($M_\odot$)	1.9±0.3	2.6±0.3

Table 2. Radial Velocities of HD 145457

JD (−2450000)	Radial Velocity (m s^{-1})	Uncertainty (m s^{-1})	Observatory
3843.85343	−31.6	6.3	Subaru
3886.92487	68.1	4.6	Subaru
3928.93366	27.9	5.4	Subaru
4554.20332	−14.7	6.2	OAO
4590.14827	71.9	5.7	OAO
4624.13390	57.5	5.6	OAO
4641.13561	14.9	5.8	OAO
4675.03053	−51.4	7.0	OAO
4754.91967	39.6	5.5	OAO
4757.91154	48.8	6.4	OAO
4758.90361	41.2	5.7	OAO
4759.90963	57.2	8.0	OAO
4835.31110	−25.6	6.3	OAO
4852.30622	−53.2	7.8	OAO
4856.36498	−61.1	7.2	OAO
4864.34776	−40.4	5.5	OAO
4883.24232	−74.1	6.0	OAO
4924.09529	35.2	6.8	OAO
4931.14786	63.2	6.2	OAO
4949.14270	92.5	6.3	OAO
4954.17821	71.7	6.8	OAO
4983.02102	25.9	6.0	OAO
5074.98880	−60.6	7.7	OAO
5133.89059	66.3	6.7	OAO
5204.34017	−54.1	6.1	OAO
5233.29591	−70.0	5.5	OAO

Table 3. Radial Velocities of HD 180314

JD (−2450000)	Radial Velocity (m s^{-1})	Uncertainty (m s^{-1})	Observatory
3844.01193	−292.1	4.3	Subaru
3887.02601	−255.7	4.2	Subaru
3929.07331	−70.4	5.2	Subaru
4560.29990	−162.5	4.9	OAO
4624.23036	−268.2	4.8	OAO
4672.12211	−281.5	4.2	OAO
4755.04398	247.9	4.0	OAO
4759.93750	296.7	4.3	OAO
4763.95272	325.1	4.7	OAO
4796.92531	387.4	3.6	OAO
4800.87738	376.4	4.2	OAO
4817.90163	334.0	4.3	OAO
4884.35171	107.6	5.0	OAO
4927.26199	−71.8	4.4	OAO
4949.26487	−143.8	4.2	OAO
4983.10598	−198.8	4.6	OAO
4983.14016	−216.7	4.4	OAO
5101.05269	−142.1	4.3	OAO
5132.01703	66.4	4.2	OAO
5160.92845	295.3	5.2	OAO
5162.89520	308.1	4.8	OAO
5182.87567	379.4	4.9	OAO
5234.38093	287.3	4.8	OAO
5267.30944	133.4	4.2	OAO

Table 4. Orbital Parameters

Parameter	HD 145457	HD 180314
P (days)	176.30±0.39	396.03±0.62
K_1 (m s^{-1})	70.6±3.1	340.8±3.3
e	0.112±0.035	0.257±0.010
ω (deg)	300±26	303.1±2.3
T_p (JD−2,450,000)	3518±13	3565.9±3.1
$a_1 \sin i$ (10^{-3}AU)	1.137±0.051	11.99±0.12
$f_1(m)$ ($10^{-7} M_\odot$)	0.0630±0.0086	14.65±0.46
$m_2 \sin i$ ($M_{\rm J}$)	2.9	22
a (AU)	0.76	1.4
$N_{\rm obs}$	26	24
rms (m s^{-1})	9.7	12.9
Reduced $\sqrt{\chi^2}$	1.8	3.1

Table 5. Bisector Quantities

Bisector Quantities	HD 145457	HD 180314
Bisector Velocity Span (BVS) (m s^{-1})	−4.9±6.3	−0.3±5.1
Bisector Velocity Curvature (BVC) (m s^{-1})	−0.2±4.0	0.3±2.2
Bisector Velocity Displacement (BVD) (m s^{-1})	−128±11	−519±12